NANO LETTERS

2008
Vol. 8, No. 3
853-858

Light Propagation within Colloidal Crystal Wire Fabricated by a Dewetting Process

Tadashi Mitsui,*,† Yutaka Wakayama,‡ Tsunenobu Onodera,§ Yosuke Takaya,§ and Hidetoshi Oikawa§

Quantum Dot Research Center, National Institute for Materials Science, Tsukuba 305-0003, Japan, Advanced Electric Materials Center, National Institute for Materials Science, Tsukuba 305-0044, Japan, and Institute of Multidisciplinary Research for Advanced Materials, Tohoku University, 2-1-1 Katahira, Aoba-ku, Sendai 980-8577, Japan

Received November 18, 2007; Revised Manuscript Received January 11, 2008

ABSTRACT

We present a colloidal crystal wire composed of thousands of connected microspheres that is fabricated by a simple dewetting process utilizing a drain phenomenon, and we directly observe the light propagation within the wire by near-field scanning optical microscopy. The optical properties of propagation light suggest that the propagation mechanism was attributed mainly to nanojet-induced mode coupling for the straight propagation component and partly to whispering-gallery mode coupling within the colloidal crystal wire.

On-chip arbitrary manipulation of a light path confined to micrometer width and extending to millimeters in length has attracted considerable attention from fundamental research and application standpoints.[1,2] However, the prevalent techniques using planar lightwave circuits require very elaborate technology to fabricate sharp bends with micrometer-scale curvature, such as air trench structure.[3] Subwavelength diameter semiconductor nanowires synthesized by laser-assisted catalytic growth are ultimate waveguides for wavelength-scale light manipulation;[4] however, the handling and assembling for lightwave circuits are still difficult. Alternatively, such sharp bends with transparent substance can be achieved by a photonic crystal concept[5–7] or by micrometer-sized resonator couplings.[8–11] In the former case, precisely defined defects can produce waveguides in photonic crystals that enable light to be guided through sharp bends, though this waveguide also requires very elaborate technology. In the latter case, light propagation through the system is attributable to the coupling between the nearest-neighbor resonators. This type of waveguide is called a coupled-resonator optical waveguide (CROW).[8,10,11] Specifically, a microsphere acts as a unique optical resonator.[11–14] One reason for this is that the whispering-gallery modes (WGMs)[8–14] within a microsphere have a transverse-magnetic polarized-type mode and a transverse-electric one; in addition, the light goes around the circumference of microspheres in the horizontal and vertical planes. Therefore, we can expect light to be guided in an arbitrary shape by connecting microspheres.

The most exact method for the alignment of microspheres should be pick-and-place robotic manipulation inside a scanning electron microscope (SEM).[15,16] However, since this bottom-up method requires the manipulation of each individual sphere, the alignment of thousands of microspheres extended over a few millimeters is an economically unrealistic process. An alternative strategy to align and connect microspheres is a method to utilize a self-assembly phenomenon in colloidal suspension.[17] In a self-assembly process, sphere−sphere interactions form an ordered structure arranged for certain kinds of dense packing, while the sphere−substrate interactions control the microsphere positions on a substrate. For example, utilization of the moving meniscus on a grooved substrate is one of the practical methods for aligning microspheres.[18–20] In this technique, microspheres in colloidal suspension regularly fall into a micrometer-scale grooved structure. However, because some etching processes to fabricate the grooved substrate can cause inevitable damage to the substrate, the etching processes are less desirable when we consider application of the CROW to optics−electronics combined-type integrated circuits.

* Corresponding author. E-mail: MITSUI.Tadashi@nims.go.jp. Tel: 81-29-863-5418. Fax: 81-29-863-5599. Correspondence should be addressed to Quantum Dot Research Center, National Institute for Materials Science, Sakura 3-13, Tsukuba, Ibaraki 305-0003, Japan.

† Quantum Dot Research Center, National Institute for Materials Science.

‡ Advanced Electric Materials Center, National Institute for Materials Science.

§ Tohoku University.

10.1021/nl073006w CCC: $40.75
Published on Web 02/06/2008

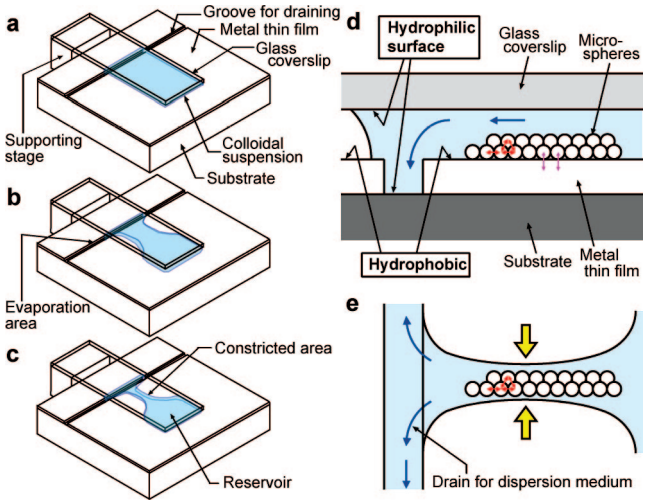

Figure 1. Fabrication of a colloidal crystal wire by the dewetting process. (a−c) Illustration of the novel fabrication technique used to fabricate the colloidal crystal wire. The technique is described in detail in later. The dewetting process proceeds from (a) to (c). (d) Profile scheme of a horizontal capillary cell. Since the bottom of the groove is hydrophilic, the suspension liquid does not retract from the substrate until the last stage of the dewetting process. (e) Plan-view scheme of (d). The movement of meniscus indicated by the yellow arrows is parallel to the groove structure in its vicinity and forms a constricted area of colloidal suspension liquid in which the microspheres are condensed during self-assembly.

Recently, a method for aligning microspheres without grooved templates has been proposed. This promising type of self-assembly is a dewetting process that controls the hydrophilic and hydrophobic properties on a substrate.[21,22] Since processes to control the hydrophilic and hydrophobic properties on a surface are easier than some etching processes, for example, hydrophobic treatment with hexamethyldisilazane (HMDS) evaporation gas, we can expect to fabricate a more complicated lightwave circuit, such as a multiplexer or displexer, conveniently.

On the other hand, to explain light propagation through a sequence of coupled microspheres, two mechanisms have been proposed: one is through the resonant coupling of WGMs,[8−14] and the other is through nanojet-induced modes (NIMs).[23,24] Kapitonov et al. demonstrated propagation losses as small as 0.5 dB per sphere in a chain of coupled microspheres.[24] However, the light path within the bundle of chains such as colloidal crystal wire was not studied in sufficient detail. If we fabricate the photonic structure within chains of coupled microspheres, we can expect to add another optical function on waveguides and lightwave circuits. In the present study, we utilized the dewetting process to align microspheres and observed the light propagation within the colloidal crystal wires in detail by using near-field scanning optical microscopy (NSOM).[25−31]

Figure 1 shows a schematic illustration of the capillary cell for fabricating a colloidal crystal wire by a dewetting process. The capillary cell was simply constructed by a single-line grooved substrate and, horizontally to the substrate's left, a glass coverslip. The first important point of the present process is that the groove structure serves not as a template but as a drain for the dispersion medium. A certain amount of the colloidal suspension was dropped onto the terrace of the substrate immediately adjacent to the coverslip from the opposite side of the supporting stage, and capillary action then drew the suspension into the cell itself. The gap between the substrate and coverslip was completely filled with suspension (Figure 1a). After that, the interface of suspension moved slowly due to the suspension drain. Note that the driving force is not the evaporation of dispersion medium in the capillary cell but the evaporation at the groove that is not covered with coverslip (Figure 1b). The utilization of drain phenomena is different from that in the process used in ref 22. In addition, since a part of the suspension is drained from the edge of the groove earlier (Figure 1d), the meniscuses, as indicated by yellow arrows, are then approached parallel to each other at the vicinity of the groove (panels c and e of Figure 1). As a result, a constricted region of suspension is formed where the microspheres are further condensed and self-assembled. The other important point in this process is the control of the hydrophilic and hydrophobic properties of the capillary cell. The hydrophobic substrate prevents the spread of the meniscus by gravitational force. On the other hand, the coverslip and the bottom of the groove structure are hydrophilic (Figure 1d). This feature holds the suspension on the substrate until the last stage of the dewetting process and maintains a uniform speed in the draining of the dispersion medium. After the dispersion medium is drained completely, the colloidal crystal wire remains.

To understand the light propagation within the colloidal wire in its entirety, we observed it by conventional optical microscopy. Figure 2a is a schematic diagram of the experimental setup. The light source used is the luminescence emitted from dye-doped fluorescent microspheres, which were illuminated and excited by violet light ($\lambda = 406$ nm) through the optical fiber probe of an NSOM, as depicted in Figure 2b. The light propagation can be visualized from the scattering in the vertical direction. On the other hand, for the measurement of the propagation light spectrum at a microsphere, observation by the guide-collection mode NSOM technique is more convenient.[28−30] The schematic diagrams of the experimental setup and the light propagation are depicted in panels c and d of Figure 2, respectively.

Figure 3a shows a typical SEM image of the colloidal crystal wire. This wire extends straight to a length of about 40 spheres or more. In addition, the microspheres included in the wire are closely connected to each other. The width of the wire is influenced by the process conditions. The most effective parameter is the gap between the coverslip and the substrate.[22] In other conditions, the microspheres build to monolayer (Figure 3b) and three layers with a pyramid-like cross section (Figure 3e). Panels c and d of Figure 3 show colloidal crystal wires which have closed-packed and tetragonal-pyramid structures, respectively. Panels f and g of Figure 3 are optical microscope images of a colloidal wire taken with and without the background white-light illumination, respectively. The vague isosceles triangle appearing near the bottom of Figure 3f is the shadow of the optical fiber probe, which is out of focus. These images reveal a

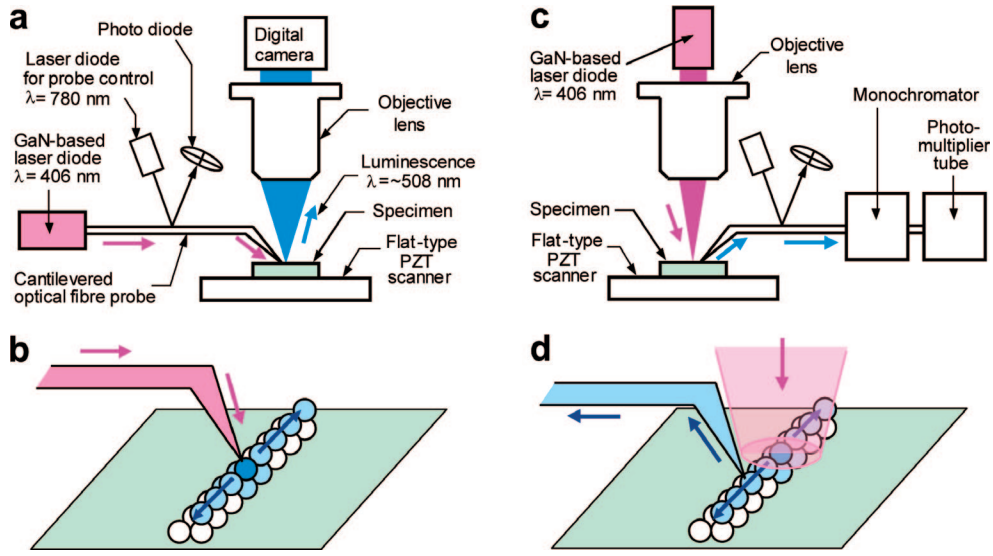

Figure 2. Observation of light propagation. (a) Experimental setup for observation by conventional optical microscopy. The excitation light is illuminated from an optical fiber probe that has an aperture at its apex. (b) Schematic illustration of emitted light propagation in (a). The luminescence emitted from the fluorescent microsphere propagates in succession through its nearest nonfluorescent neighbors. (c) Experimental setup of guide-collection mode NSOM. (d) Light propagation in (c). In guide-collection mode, the propagated light is collected through a fiber probe.

luminescent microsphere on the edge of the bottom layer. Figure 3g shows that the luminescence emitted from it strongly propagates to the upper layer along two directions in which the microspheres are aligned straight. Figure 3h shows the plan-view schematic illustration of the colloidal wire and the light paths within it. In horizontal directions, though light can propagate to the directions across and parallel to the wire, light cannot propagate to the diagonal directions because the wire has a tetragonal lattice structure and the microspheres do not make contact with each other. On the other hand, we should note that the light propagated to the microspheres at the opposite side in the second layer; in other words, the light climbs down the pyramid. Moreover, part of the light propagates parallel to the wire. This suggests there is some scattering or bending of light within the microsphere in the top layer.

To evaluate the light propagation through nearest-neighbor microspheres in succession, we observed a longer wire. Panels a and b of Figure 4 are optical microscope images of the wire taken with and without the illumination, respectively, as in panels f and g of Figure 3. SEM observation (data not shown) revealed that the colloidal wire consists of two layers, and the structure is a tetragonal-pyramid lattice as shown in inset of Figure 4a. Figure 4a shows that there is a luminescent microsphere in the upper layer of the colloidal wire, and Figure 4b shows that the luminescence emitted from it propagates parallel to the wire. The line profile of green light intensity along the upper layer is shown in Figure 4c. This profile indicates that the luminescent light propagates to the sphere at a distance of 44 μm (22 spheres; indicated by B) from the original luminescent sphere. To study propagation loss through the colloidal crystal wire, we found the maxima of the intensity and calculated the dependence of attenuation as in ref 24. The attenuation curve fits well to a double-exponential function

$$I = 10^{-0.1\beta_1 N} I_1 + 10^{-0.1\beta_2 N} I_2 \quad (1)$$

where I_1 and I_2 are intensities of two exponential components, β_1 and β_2 are their attenuation constants per individual sphere (in dB), and N is the propagation distance expressed in the number of spheres.[24] In Figure 4c, β_1 and β_2 are about 1.8 and 0.4, and these are comparable to the results within an individual straight line ($\beta_1 \approx 2.0$ and $\beta_2 \approx 0.5$).[24] From this, the NIMs coupling is the most likely mechanism of the straight component of light propagation through the colloidal crystal wire. In addition, $\beta_2 = 0.4$ (dB/per individual sphere) is equal to $\beta_2 = 2.0$ (dB/10 μm). When we use the colloidal crystal wire as a waveguide, this value is between that of CdS nanowire (1.0 dB/10 μm) and InGaAs-based waveguide (2.3 dB/10 μm).[4]

Figure 4d shows the spectrum of the propagation light taken at point A by means of the guide-collection-mode NSOM technique (Figures 2c and 2d). The spectrum plotted by the blue line is that of propagation light, and that in red is the luminescence spectrum of fluorescent microspheres dispersed in water for reference. The spectrum plotted by the red line shows the spectrum of the dye itself. The spectrum of propagation light shows periodic peaks, and indicates that there are some resonance structures within the microspheres.[9–11] This result suggests that the resonance of WGMs should also be associated with the mechanism of light propagation. Chen et al. have calculated optical transport through a bent chain of microspheres by means of the generalized multiparticle Mie theory, which includes NIM and WGM couplings.[9] They revealed that efficient WGM coupling can take place even across the abrupt direction change of 90°. Though the quality of microspheres in this article is not so good for propagation by WGM coupling,[12]

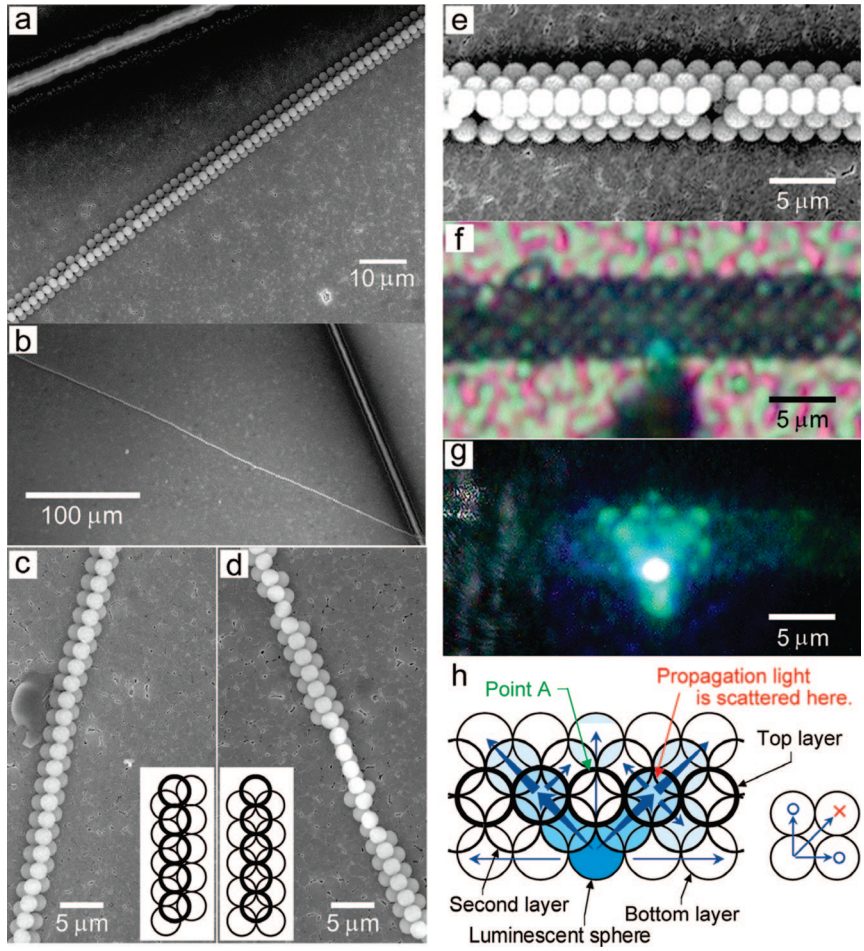

Figure 3. Scanning electron microscope images of colloidal crystal wires and light propagation within it. (a−d) Typical SEM images of the colloidal crystal wires. (a) The microspheres are aligned nearly straight over a length of 80 μm. The colloidal crystal wire is composed of four lines of aligned microspheres and extends about 2 mm beyond the left of this micrograph. The groove structure is shown on the upper left side of the micrograph. To increase the wire length, a glass coverslip was set at an angle of 10° from the groove. (b) The microspheres are aligned in a line. (c, d) Closed-packed lattice and tetragonal-packed lattice of microspheres, respectively. (e) SEM image of the colloidal crystal wire consists of three layers. It has a pyramid-like cross section. (f, g) Optical microscope images of the colloidal crystal wire taken at the same region with and without the background white-light illumination, respectively. The structure of the colloidal wire shown in these images is the same as shown in Figure 3e, but the region is not the same. (h) Plan-view schematic illustration of the colloidal wire and the light path within it. The green luminescence light does not propagate to the microsphere in the top layer indicated as Point A.

the "quasi"-WGM coupling between detuned spherical cavities should make broad spectral transmission as predicted by Kanaev et al.[10] Therefore, WGM coupling should fulfill an important role for light propagation at the bending point within the colloidal crystal wire.

In conclusion, the dewetting process developed in the present study successfully provided a very long colloidal crystal wire composed of thousands of microspheres in close contact with each other on a plain substrate. The propagation mechanism was attributed mainly to NIM coupling for the straight propagation component and partly to WGM coupling at the bending place within the colloidal crystal wire.

Methods. Sample Fabrication. The groove structure (Figure 1) used to drain the dispersion medium from the colloidal suspension was fabricated by a reactive ion etching process after photolithographical patterning on a 4-μm-thick aluminum/20-nm-thick chromium film grown on a glass substrate. The groove width was 6 μm. The coverslip of horizontal capillary cells depicted in panels a−c of Figure 1 was fixed using acrylic adhesives on the supporting stage across the groove structure. The gap between the coverslip and the substrate was less than 100 μm. The coverslip was cut to a few millimeters in width and restricted the colloidal suspension within narrow limits. The colloidal suspension was obtained from Duke Scientific Corp. (Palo Alto, CA). The suspension contains microdispersed polystyrene microspheres (2.001 ± 0.025 μm in diameter, 1.1% variation coefficient, with a density of 1.05 g cm^{-3} and refractive index of 1.59 at 589 nm). The fluorescent microspheres were also made of polystyrene and were green-dyed with a wavelength emission maximum of 508 nm. The mean diameter of the fluorescent microspheres was nearly equal to that of the nonfluorescent microspheres. The fluorescent microspheres were combined with the nonfluorescent microspheres by mixing the two suspensions at a mixing ratio of 1:400. The mean diameter of the microspheres was certified by the National Institute of Standards and Technology (NIST). All dewetting processes were performed at room temperature (22

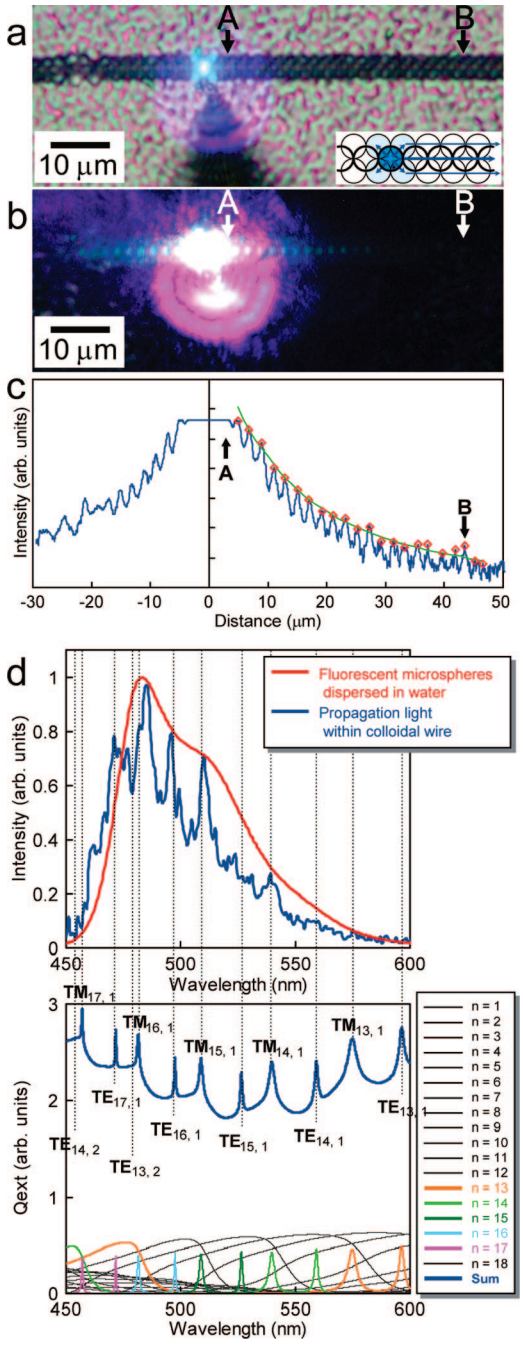

Figure 4. Propagation loss and spectrum of the propagation light through a colloidal crystal wire. (a, b) Optical microscope images of the colloidal crystal wire with and without the background white-light illumination, respectively. Although the excitation light looks rather strong in this digital camera image, the propagation of green luminescence light can be sufficiently observed even by the naked eye. (c) Line profile of the light intensity along the upper layer (blue). This profile indicates that the luminescent light propagates to the sphere at a distance of 44 μm (22 spheres; indicated by B) from the original luminescent sphere. The green line is fitted with a double-exponential function of distance. (d) Spectra of propagated light taken at point A (blue) and luminescence of fluorescent microspheres dispersed in water (red). The peaks in the spectrum of propagation light show a relatively good correspondence with the results calculated using the Mie theory as indicated in the figure below.

°C). The humidity was kept above 40% and under 60% by using a cover case. In this condition, evaporation is slower than that observed under the condition of ref 22 (in which the humidity was 33%). The typical contact angle between Al_2O_3 and water is 30° although that between SiO_2 and water is 8°. In addition, the contact angle between aluminum and water is 92°.

Observation of Light Propagation. The scattered light, which is a part of the propagation light shown in panels f and g of Figure 3 and panels a and b of Figure 4, was collected by a long-working-distance objective lens (SLWD L Plan 50×, Nikon Corp., Tokyo, Japan) and was detected by a conventional digital camera. To excite fluorescent microspheres, the 406-nm laser light from a GaN-based semiconductor laser diode (Neoark Corp., Hachioji, Japan) was illuminated using an optical fiber probe fabricated from a multimode optical fiber by melting and pulling techniques (Nanonics Imaging Ltd., Jerusalem, Israel). The nominal aperture size was 200 nm. One reason this probe was chosen is that it can illuminate only one sphere through the small aperture at its apex; the subwavelength spatial resolution of NSOM derives its origin from this small aperture. Additionally, the fiber probe can dramatically suppress the scattering light because the difference in the refractive indices between the sphere (polystyrene, 1.59) and the fiber probe (silica glass, 1.49) is smaller than that between the sphere and air. If the violet light is directly incident to the fluorescent microsphere by the objective lens, the scattering light from the microsphere becomes too strong for the luminescence that propagates through the colloidal crystal wire to be observed. The fiber probe was bent, and equipped with the NSOM (MultiView 1000, Nanonics Imaging Ltd.)[31] as a cantilever. The distance between the probe and the specimen was kept constant by a tapping-mode feedback system. The intensity profile indicated in Figure 4c was plotted using the green component extraction from Figure 4b.

Acknowledgment. This study was carried out as a collaborative project between the Institute of Multidisciplinary Research for Advanced Materials of Tohoku University and the National Institute for Materials Science (NIMS), as well as in conjunction with the Active Nano-Characterization and Technology Project. It was supported financially by Special Coordination Funds from the Ministry of Education, Culture, Sports, Science, and Technology of the Japanese Government. This work was partly supported by Grant-in-Aid for Scientific Research (B) (19310092) of the Japanese Government. The authors thank Dr. H. T. Miyazaki for fruitful discussions.

References

(1) Almeida, V. R.; Barrios, C. A.; Panepucci, R. R.; Lipson, M. *Nature* **2004**, *431*, 1081–1084.
(2) Hill, M. T.; Dorren, H. J. S.; de Vries, T.; Leijtens, X. J. M.; den Besten, J. H.; Smalbrugge, B.; Oei, Y. -S.; Binsma, H.; Khoe, G. -D.; Smit, M. K. *Nature* **2004**, *432*, 206–209.
(3) Akiyama, S.; Popovic, M. A.; Rakich, P. T.; Wada, K.; Michel, E.; Haus, H. A.; Ippen, E. P.; Kimerling, L. C. *J. Lightwave Technol.* **2005**, *23*, 2271–2277.
(4) Barrelet, C. J.; Greytak, A. B.; Lieber, C. M. *Nano Lett.* **2004**, *4*, 1981–1985.
(5) Mekis, A.; Chen, J. C.; Kurland, I.; Fan, S.; Villeneuve, P. R.; Joannopoulous, J. D. *Phys. Rev. Lett.* **1996**, *77*, 3787–3790.
(6) Joannopoulous, J. D.; Villeneuve, P. R.; Fan, S. *Nature* **1997**, *386*, 143–149.

(7) Talneau, A.; Le Gouezigou, L.; Bouadma, N.; Kafesaki, M.; Soukoulis, C. M.; Agio, M. *Appl. Phys. Lett.* **2002**, *80*, 547–549.
(8) Yariv, A.; Xu, Y.; Lee, R. K.; Scherer, A. *Opt. Lett.* **1999**, *24*, 711–713.
(9) Chen, Z.; Taflove, A.; Backman, V. *Opt. Lett.* **2006**, *31*, 389–391.
(10) Kanaev, A. V.; Astratov, V. N.; Cai, W. *Appl. Phys. Lett.* **2006**, *88*, 111111.
(11) Möller, B. M.; Woggon, U.; Artemyev, M. V. *Opt. Lett.* **2005**, *30*, 2116–2118.
(12) Hara, Y.; Mukaiyama, T.; Takeda, K.; Kuwata-Gonokami, M. *Phys. Rev. Lett.* **2005**, *94*, 203905.
(13) Conwell, P. R.; Barber, P. W.; Rushforth, C. K. *J. Opt. Soc. Am.* **1984**, *A 1*, 62–67.
(14) Benner, R. E.; Barber, P. W.; Owen, J. F.; Chang, R. K. *Phys. Rev. Lett.* **1980**, *44*, 475–478.
(15) Garcia-Santamaria, F.; Miyazaki, H. T.; Urquia, A.; Ibisate, M.; Belmonte, M.; Shinya, N.; Meseguer, F.; Lopez, C. *Adv. Mater.* **2002**, *14*, 1144–1147.
(16) Aoki, K.; Miyazaki, H. T.; Hirayama, H.; Inoshita, K.; Baba, T.; Sakoda, K.; Shinya, N.; Aoyagi, Y. *Nat. Mater.* **2003**, *2*, 117–121.
(17) van Blaaderen, A.; Ruel, R.; Wiltzius, P. *Nature* **1997**, *385*, 321–324.
(18) Yin, Y.; Lu, Y.; Gates, B.; Xia, Y. *J. Am. Chem. Soc.* **2001**, *123*, 8718–8729.
(19) Kraus, T.; Malaquin, L.; Delamarche, E.; Schmid, H.; Spencer, N. D.; Wolf, H. *Adv. Mater.* **2005**, *17*, 2438–2442.
(20) Grego, S.; Jarvis, T. W.; Stoner, B. R.; Lewis, J. S. *Langmuir* **2005**, *21*, 4971–4975.
(21) Wang, J. Z.; Zheng, Z. H.; Li, H. W.; Huck, W. T. S.; Sirringhaus, H. *Nat. Mater.* **2004**, *3*, 171–176.
(22) Vyawahare, S.; Craig, K. M.; Scherer, A. *Nano Lett.* **2006**, *6*, 271–276.
(23) Chen, Z.; Taflove, A.; Backman, V. *Opt. Express* **2004**, *12*, 1214–1220.
(24) Kapitonov, A. M.; Astratov, V. N. *Opt. Lett.* **2007**, *32*, 409–411.
(25) Pohl, D.; Denk, W.; Lanz, M. *Appl. Phys. Lett.* **1984**, *44*, 651–653.
(26) Durig, U.; Pohl, D.; Rohner, F. *J. Appl. Phys.* **1986**, *59*, 3318–3327.
(27) Lewis, A.; Isaacson, M.; Harootunian, A.; Muray, A. *Ultramicroscopy* **1984**, *13*, 227–231.
(28) Tsai, D. P.; Jackson, H. E.; Reddick, R. C.; Sharp, S. H.; Warmack, R. J. *Appl. Phys. Lett.* **1990**, *56*, 1515–1517.
(29) Bourzeix, S.; Moison, J. M.; Mignard, F.; Barthe, F.; Boccara, A. C.; Licoppe, C.; Mersali, B.; Allovon, M.; Bruno, A. *Appl. Phys. Lett.* **1998**, *73*, 1035–1037.
(30) Mitsui, T. *Rev. Sci. Instrum.* **2005**, *76*, 043703.
(31) Lieberman, K.; Ben-Ami, N.; Lewis, A. *Rev. Sci. Instrum.* **1996**, *67*, 3567–3572.

NL073006W